N = 16 subshell closure from stability to the neutron drip line

A. Obertelli[1], S. Péru[2], J.-P. Delaroche[2], A. Gillibert[1], M. Girod[2], H. Goutte[2]
[1] *CEA-SACLAY, DSM/DAPNIA/SPhN, F-91191 Gif-sur-Yvette, France*
[2] *CEA/DIF/DPTA/SPN, B.P. 12, 91680 Bruyères-le-Châtel, France*

(Dated: Received: date/ Revised version: date)

The Hartree-Fock-Bogoliubov method implemented with the Gogny D1S force and used in a systematic study of the even-even N = 16 isotones from stability to the neutron drip line strongly suggests that a subshell gap, approximately 4 MeV wide, is opening at N = 16. First 2^+ levels as well as $B(E2; 0^+_{gs} \rightarrow 2^+)$ reduced $E2$ transition probabilities have also been predicted in configuration mixing and standard Random Phase Approximation calculations using D1S. These results compare favorably with experimental information available for the Z = 10 - 18 nuclei and with expectations for ^{24}O properties. They also fully support our mean-field predictions, namely that N = 16 is a spherical magic number at the oxygen neutron drip line.

PACS numbers: 21.60.Ev, 21.60.Jz, 21.10.Re, 21.10.Ky

I. INTRODUCTION

One of the most striking evidence for quantum mechanics in physics is the existence of magic numbers. From atomic physics to nuclear physics, they are associated to a shell structure and a spherical configuration for which all the available individual levels are filled. In atomic physics, the rare gas are well known examples of enhanced stability in their chemical properties. In nuclear physics, the same situation indeed occurs but for magic numbers different from those found in atomic physics. The sequence of magic numbers for stable nuclei was explained theoretically for the first time fifty years ago [1, 2], and is now well understood. The properties of magic nuclei like ^{40}Ca or ^{208}Pb were extensively studied and are the first observables to validate the shell model picture. However, the magnitude of shell gaps may evolve from stability towards drip lines. It may decrease, as already observed at the neutron number N = 20 for which spherical magicity vanishes at the neutron drip line [3]. This magnitude may increase as well, and give rise to a new magic number at the drip line, not observed for stable nuclei. Recent experimental investigations far away from the valley of stability highlight modifications in the shell model structure. Several observables show that N = 16 neutron rich isotones present a higher stability compared to their neighbours in the N-Z chart, namely
i) the N = 16 isotones ^{22}C, ^{23}N, and ^{24}O are the last bound nuclei of their respective isotopic chains [4, 5],
ii) the large energy gap around the Fermi surface for the N = 16 ^{28}Mg and ^{26}Ne nuclei causes a break in the neutron separation energy S_n systematics, and
iii) the first 2^+ level of ^{24}O has been suggested in a recent γ-spectroscopy experiment [6] to lie at higher excitation energy than the one neutron separation threshold S_n = 3.7 MeV [7]. Such an excitation energy is much higher than the experimental $E(2^+)$'s observed for the other oxygen isotopes.
For these reasons, N = 16 is proposed to be a magic number for the most neutron rich isotones [8]. This means an enhancement of the spherical gap between the $s_{1/2}$ and the $d_{3/2}$ subshells of the neutron *sd* shell compared to its value for stable nuclei [9–11].
In this paper, we study N = 16 as a possible new spherical magic number for neutron rich nuclei. Our approach mainly relies on the Hartree-Fock-Bogoliubov (HFB) method. We show that the shell evolution may be interpreted and quantitatively reproduced with the Gogny-D1S effective interaction [12, 13]. Self-consistent mean-field methods [14, 15] have already been used to study light nuclei. In a previous work [16], the evolution from the stability region to the neutron rich isotopes of the N = 20 and N = 28 shells has been discussed. Here, we study the N = 16 isotones from ^{22}C, at the neutron drip line, to ^{34}Ar through a systematic description of even-even nuclei. Axial and triaxial deformations are investigated.
In the following, we briefly recall the HFB formalism and notations. The results from pure mean-field calculations restricted to axial symmetry are presented as a first step. Pairing energies are discussed. Extending the HFB calculations to triaxial shapes, collective 2^+ levels and reduced transition probabilities $B(E2)$'s are derived from the Generator Coordinate Method (GCM) implemented within the Gaussian Overlap Approximation (GOA). This configuration mixing approach complements the mean-field description and also points to N = 16 as a spherical neutron magic number far away from the stability line. Finally, standard Random Phase Approximation (RPA) calculations using the same effective force are performed for ^{24}O.

II. MEAN-FIELD DESCRIPTION

In the constrained HFB theory, the deformed states $|\Phi_q>$ of a nucleus are described as quasiparticule (qp) vacua. The $|\Phi_q>$ states are deduced from the minimization of the energy functional

$$\delta < \Phi_q|\hat{H} - \lambda_N\hat{N} - \lambda_Z\hat{Z} - \sum_i \lambda_i\hat{Q}_i|\Phi_q >= 0, \quad (1)$$

where $|\Phi_q>$ is the HFB wave function of deformation q, and $\hat{H}$ is the many-body nuclear Hamiltonian. In this study, the finite range Gogny-D1S interaction is used, and both mean and pairing fields are calculated in a consistent way. The λ's in Eq. 1 are the Lagrange multipliers associated with the constraints on nucleon numbers N and Z and average deformations Q_i :

$$\begin{aligned} < \Phi_q|\hat{N}|\Phi_q >= N, \\ < \Phi_q|\hat{Z}|\Phi_q >= Z, \\ < \Phi_q|\hat{Q}_i|\Phi_q >= Q_i\,. \end{aligned} \quad (2)$$

The $\hat{Q}_i$'s are taken as the quadrupole operators $\hat{Q}_{20}$ and $\hat{Q}_{22}$, related to the axial and triaxial Bohr deformations β and γ :

$$\beta = \sqrt{\frac{\pi}{5}}\frac{\sqrt{(Q_{20}^2 + 3Q_{22}^2)}}{AR^2},\ \gamma = \arctan\frac{\sqrt{3}Q_{22}}{Q_{20}}, \quad (3)$$

where A and R = $\sqrt{\frac{3}{5}}\left(1.2A^{1/3}\right)$ (fm) are the mass number and radius of the nucleus under consideration, respectively.

We first investigate within constrained axial calculations the N = 16 isotones to test their magicity. At this stage, we consider that neutron (proton) magicity occurs when two criteria are fulfilled : *i)* the nucleus is spherical: the potential energy is minimum at zero deformation, and *ii)* a large energy gap separates the levels above and below the Fermi surface. The second condition is satisfied when the neutron (proton) pairing energy cancels at zero deformation in this pure mean-field description. In the HFB formalism, the neutron (proton) pairing energy is given by $E_{n(p)} = \frac{1}{2}Tr\Delta\kappa$, where Δ and κ are the pairing field and the pairing tensor, respectively [17]. Such a correlation energy *is not* the net gain between the HFB and HF treatments. However, when the pairing field vanishes, HF and HFB descriptions give rise to the same total potential energy and no correlation energy is found at the mean field level. Consequently, the study of pairing energies $E_{n(p)}$ provides direct information about pairing correlations.

In the present work, the mean-field equations are solved using basis sets of deformed harmonic oscillators including $N_0 = 9$ major shells. Such a large basis ensures stability of level energies at all deformations up to $\beta \simeq 1$. As an example, Fig. 1 illustrates the convergence of the neutron pairing energy E_n and the potential energy

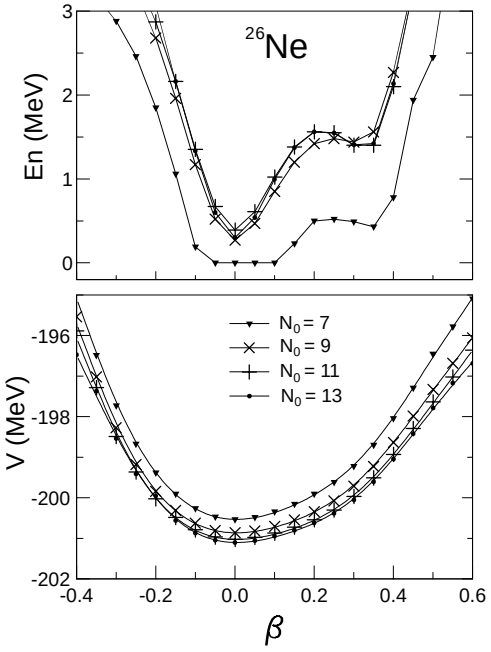

FIG. 1: Neutron pairing energies E_n (upper panel) and potential energy surfaces V (lower panel) of ^{26}Ne for different basis sizes as functions of the axial deformation parameter β. The numbers of major shells considered are N_0 = 7, 9, 11, and 13.

$V =< \Phi_q|\hat{H}|\Phi_q >$ for ^{26}Ne with the basis size increasing from $N_0 = 7$ to $N_0 = 13$. Calculations with $N_0 = 7$ clearly do not reach the convergence, whereas those with $N_0 = 9$, 11, and 13 give the same results within 400 keV for V and 200 keV for E_n. Then, a reasonable convergence is achieved for $N_0 = 9$. This result holds true for all the other isotones under study.

All the axial potential energy surfaces (PESs) of the N = 16 isotones, shown in Fig. 2, display a minimum at $\beta = 0$. Thus, the first criterium *(i)* for magicity is fulfilled for all isotones at the pure mean-field level. Nevertheless, this minimum is shallow for the nuclei from ^{26}Ne to ^{34}Ar and their neutron pairing energies, shown in Fig. 3, do not vanish at zero deformation. According to criterium *(ii)*, these nuclei are not magic. The neutron pairing energy vanishes at $\beta = 0$ only for ^{24}O and ^{22}C. Then, criteria *(i)* and *(ii)* are simultaneously verified only for these two nuclei, which are predicted to be magic. Furthermore, proton pairing energy vanishes at $\beta = 0$ for ^{24}O which is then found to be doubly magic.

A gradual evolution is observed in Fig. 3 for the neutron pairing energy : neutron pairing energy goes to zero around $\beta \simeq 0.4$ for ^{34}Ar, ^{32}S, and ^{30}Si. ^{32}S presents a shoulder at $\beta = 0$. Moving toward the drip line, this shoulder gets more pronounced and becomes a local minimum for ^{30}Si, ^{28}Mg and ^{26}Ne. The neutron pairing energy vanishes at $\beta = 0$ for ^{24}O and ^{22}C. The evolution of these two pairing energy minima is directly linked to

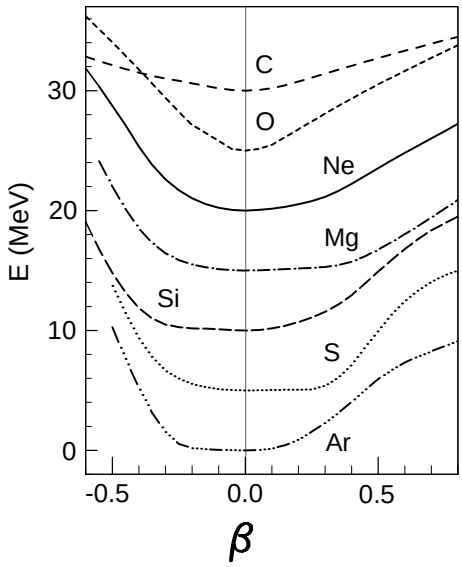

FIG. 2: Potential energy surfaces of the N = 16 isotones from Argon to Carbon, as functions of the axial deformation parameter β. The minimum potential energy for Argon is set to zero. The minima of the curves are arbitrarily separated by 5 MeV. Stable nuclei are ^{32}S and ^{30}Si.

the existence of prolate and spherical gaps between the $K^\pi = 1/2^+$ orbitals – where K is the projection of the angular momentum on the intrinsic symmetry axis –, from the $s_{1/2}$ and $d_{3/2}$ neutron subshells. This subshell structure is shown in the lower panel of Fig. 4 for ^{32}S and ^{26}Ne. While ^{32}S has a 6 MeV wide prolate gap and a 3.3 MeV wide spherical gap, ^{26}Ne presents an inverse trend : these gaps are 3.5 MeV and 4.2 MeV wide, respectively.

On top of Fig. 4 is shown the opening of the spherical gap δ between the $s_{1/2}$ and $d_{3/2}$ neutron subshells for nuclei from Z = 18 to Z = 6. For ^{24}O, this gap is $\delta \simeq 4$ MeV wide. To check the stability of this prediction, δ has also been calculated using the older D1 [12] parametrization of the Gogny force. The results do not depend significantly on the force parametrization (see table I). The difference between the two calculations does not exceed 600 keV for δ. Both D1 and D1S parametrizations lead to the prediction of N = 16 as magic number at the neutron drip line.

TABLE I: Spherical energy gap δ between the $s_{1/2}$ and $d_{3/2}$ subshells at $\beta = 0$ predicted using the D1S and D1 interactions in HFB calculations.

		^{34}Ar	^{32}S	^{30}Si	^{28}Mg	^{26}Ne	^{24}O	^{22}C
D1S	δ (MeV)	2.58	3.32	4.00	4.11	4.25	4.30	4.75
D1	δ (MeV)	2.33	2.89	3.24	3.53	3.87	4.17	4.74

To summarize, N = 16 is predicted to be a spherical magic number at the neutron drip line for ^{24}O and ^{22}C in a pure mean-field approach. It preexists as a strong shell effect in nuclei of the stability region.

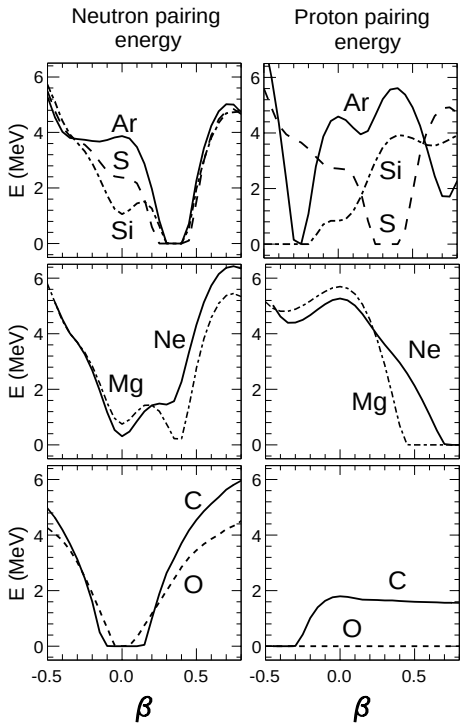

FIG. 3: Neutron (left) and proton (right) pairing energy curves for N = 16 isotones from Argon to Carbon, as functions of the axial deformation parameter β.

III. BEYOND THE MEAN-FIELD

To complement the description of these nuclei, an approach beyond the mean field is considered. A dynamical description of the ground-state and low lying 2^+ collective state is derived from GCM considering rotational and vibrational degrees of freedom in the triaxial plane. Collective states are taken as linear combinations of constrained HFB basis states $|\Phi_q>$, namely

$$|\Psi_k> = \int dq\, f_k(q)\, |\Phi_q> \ . \qquad (4)$$

Here, q is a 5-dimensional generator coordinate : two dimensions (β, γ) for vibrations and three Euler angles for rotation, and $f_k(q)$ are weight functions, solutions of the Hill-Wheeler equation [18]. The Gaussian Overlap Approximation transforms the integro-differential Hill-Wheeler equation into a computationally tractable Schrödinger-like equation [19] :

$$\hat{\mathcal{H}}_{coll}\, g_k(q) = E_k\, g_k(q), \qquad (5)$$

where $g_k(q)$ is the Gauss transform of $f_k(q)$ and eigenstate of the collective Hamiltonian $\hat{\mathcal{H}}_{coll}$ [20, 21].

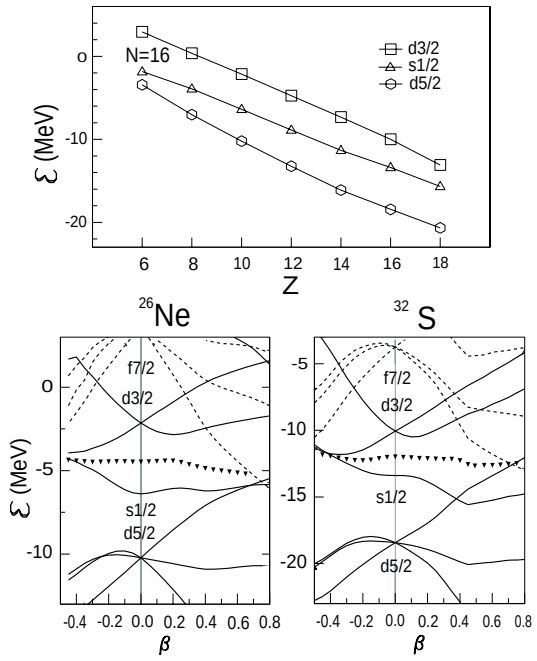

FIG. 4: Upper panel : Neutron single particle energies for even-even N = 16 isotones at $\beta = 0$. Lower panel : Neutron individual levels around the Fermi surface of ^{32}S (left) and ^{26}Ne (right) as functions of the axial deformation parameter β. Triangles represent the chemical potential.

TABLE II: First 2^+ level and $B(E2; 0^+_{gs} \rightarrow 2^+)$ properties of even-even N = 16 isotones. J^A inertia parameters are adopted in the configuration mixing calculations for Z = 10 - 18 nuclei (see text). Standard RPA predictions usind D1S are given for ^{24}O. Experimental data are from [28].

	$<\beta>$		$E(2^+)$		$B(E2; 0^+_{gs} \rightarrow 2^+)$	
	g.s.	2^+	(MeV)		(e^2fm^4)	
	th.		th.	exp.	th.	exp.
^{34}Ar	0.27	0.31	1.98	2.09	306	240(40)
^{32}S	0.31	0.32	1.78	2.23	254	300(13)
^{30}Si	0.32	0.37	2.11	2.23	220	215(10)
^{28}Mg	0.39	0.43	1.50	1.47	202	350(5)
^{26}Ne	0.31	0.37	2.19	2.02	86	228(41)
^{24}O	-	-	3.81	-	15	-

It is a wide spread practice to perform calculations of mass and inertia parameters using the Inglis and Beylaev approximation [22, 23]. This sounds to be a reasonable assumption at low spin and excitation energy only for medium and heavy mass nuclei. As it has been shown recently, improvements over the Belyaev formula for moments of inertia were necessary to provide a good description of ^{40,42,44}S low energy spectra [24]. In the present work focusing on still lighter mass nuclei, two sets of moments of inertia $J^A_{x,y,z}$ and $J^B_{x,y,z}$ have been calculated over the (β,γ) plane as follows. In the first set, $J^A_{x,y,z}$ is

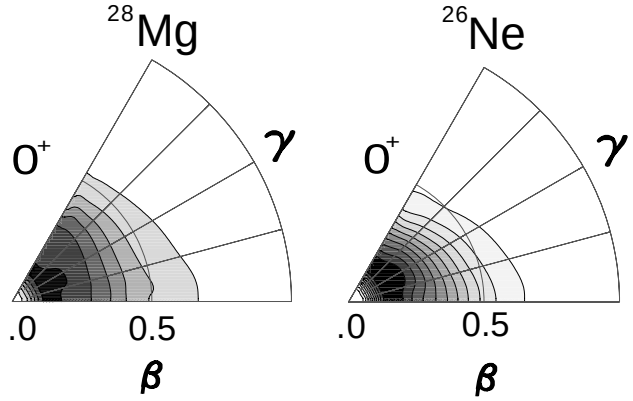

FIG. 5: Collective wave functions of the ^{26}Ne and ^{28}Mg ground-states in the (β, γ) triaxial plane.

defined as

$$J^A_{x,y,z} = \frac{< \Phi_{q,\omega_{x,y,z}} | \hat{I}_{x,y,z} | \Phi_{q,\omega_{x,y,z}} >}{\omega_{x,y,z}}, \qquad (6)$$

where $\hat{I}_{x,y,z}$ are the angular momentum projections in the intrinsic system of coordinates x, y, and z, and $\omega_{x,y,z}$ the associated rotational frequencies for a nucleus with rotational energy E(I). First, J^A_z is calculated from minimization of the energy functional $< \Phi_{q,\omega_z} | \hat{H} - \lambda_N \hat{N} - \lambda_Z \hat{Z} - \omega_z \hat{I}_z | \Phi_{q,\omega_z} >$ in the rotating frame [25], with the additional constraint $< \Phi_{q,\omega_z} | \hat{I}_z | \Phi_{q,\omega_z} > = \hbar^2 \sqrt{I(I+1)}$. Here we use I = 2. The moments J^A_x and J^A_y are then calculated after permutation of the principal axes. Finally, the second set $J^B_{x,y,z}$ results from using the Thouless-Valatin approximation [26], namely

$$J^B_{x,y,z} = \lim_{\omega_{x,y,z} \rightarrow 0} \frac{< \Phi_{q,\omega_{x,y,z}} | \hat{I}_{x,y,z} | \Phi_{q,\omega_{x,y,z}} >}{\omega_{x,y,z}}. \qquad (7)$$

Equations 6 and 7 form two prescriptions for calculating moments of inertia. Each prescription has been tested separately while solving $\hat{\mathcal{H}}_{coll}$, and their figure of merit is discussed below. Using the configuration mixing method outlined above, we find that ^{24}O and ^{22}C are spherical in their ground states whereas all the others from ^{34}Ar to ^{26}Ne are deformed. An illustration is provided for ^{26}Ne and ^{28}Mg in Fig. 5 where are shown their ground state wave functions over the (β, γ) coordinates. The topology of these surfaces suggests γ-unstable deformed shapes with mean quadrupole deformations $< \beta > = 0.31$ and 0.39, and $< \gamma > = 24^\circ$ and 22° for ^{26}Ne and ^{28}Mg, respectively. This illustration provides a posteriori justification for our method in which the five collective quadrupole coordinates are explicitly treated.

The first 2^+ level energy and the $B(E2;0^+_{gs} \rightarrow 2^+)$ reduced transition probability values calculated with J^A and J^B moments of inertia as collective model inputs are shown in Fig. 6 as open circles and stars, respectively, for the N = 16 isotones from Z = 10 to Z = 18. Standard RPA calculations [27] have also been performed for the doubly magic ^{24}O nucleus using the Gogny-D1S force. In Fig. 6, RPA results (squares) are shown for completeness. Table II includes most of these predictions as well as experimental data [28] and mean deformations. As can be seen in the upper part of Fig. 6, the two sets of predictions for E(2^+) (i.e. stars and open circles) significantly differ from each other, the differences being at a maximum for Z = 10 and Z = 12. On the other hand, as expected, the improvement in our determination of moments of inertia leads to bring the E(2^+) predictions marked by open circles in close agreement with each measured value (triangles) and with the pattern they display as Z increases from Z = 10 to Z = 18. The lowering observed for the 2^+ level in ^{28}Mg is here interpreted as stemming from a stronger mean deformation (see Table II).

The experimental information available on the ^{24}O structure is rather scarce. In recent in-beam γ-ray spectroscopy measurements [6], the $2^+ \rightarrow 0^+_{gs}$ γ-decay was not observed, feature suggesting that the first 2^+ excited state lies above the neutron decay threshold S_n = 3.7 MeV. An excitation energy E(2^+) $\geq$ 3.7 MeV would roughly be two times higher than those for the Z = 10 - 18 members of the N = 16 isotonic chain, and would be consistent with the present RPA prediction $E(2^+)$ = 3.81 MeV. These results together with those described above for the Z = 10 - 18 members of the N = 16 isotonic chain points to the existence of a subshell closure at the oxygen neutron drip line.

IV. CONCLUSION

In this paper, a systematic structure study of the even-even N = 16 isotones has been performed from stability to the neutron drip line. This has been achieved at both mean-field and configuration mixing levels using the Gogny-D1S effective interaction. Standard RPA calculations have also been performed for ^{24}O to complement our survey. These methods allow us to investigate single-particle and pairing properties at spherical shape and along axial and triaxial quadrupole deformations, as well as collective properties.

The mean-field calculations show that a spherical subshell gap is opening at N = 16 (see Fig. 4). Its size ($\delta \simeq 4$ MeV) does not significantly depend on whether the D1 or D1S parametrization of the Gogny force is used. Furthermore the neutron pairing energy at spherical shape vanishes only for ^{24}O and ^{22}C. Since the potential energy surfaces of these nuclei also show a minimum at zero deformation, we conclude that N = 16 is a magic number at the neutron drip line, that is for ^{24}O and ^{22}C.

Results from configuration mixing calculations bring confirmation that both nuclei are spherical in their ground states. In contrast similar calculations suggest that all the Z = 10 - 18 isotones show strong mean deformations. A new prescription taylored to calculate moments of inertia in light nuclei leads to improved E(2^+) and $B(E2;0^+_{gs} \rightarrow 2^+)$ predictions that are in good overall agreement with experimental data available for the Z = 10 - 18 nuclei. Our predictions suggest that i) collectivity of the $0^+_{gs} \rightarrow 2^+$ transitions gradually decreases as Z gets away from Z = 18 and reaches a minimum at Z = 8, where it is 20 times weaker than at Z = 18, and ii) E(2^+) energies raise sharply from 1.98 MeV (^{34}Ar) to 3.81 MeV (^{24}O). These collective properties are strongly suggestive of N = 16 as magic number at the neutron drip line.

Experimental determination of the 2^+ excitation energy for ^{24}O is needed to challenge the reliability of our model predictions based on Gogny D1S force. It is now a key issue to precisely understand the reasons why this force is providing a subshell gap at the N = 16 neutron drip line. Work along this line is in progress.

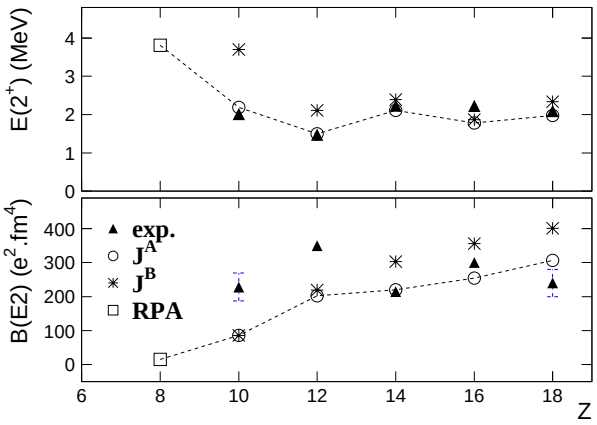

FIG. 6: Upper panel : Energies of the first 2^+ excited state for even-even N = 16 isotones from Z = 18 to Z = 8. Lower panel : Reduced transition probabilities $B(E2;0^+_{gs} \rightarrow 2^+)$. Experimental data (triangles) are available down to Z = 10. Both calculations with J^A (open circles) and J^B (stars) are represented from Z = 18 to Z = 10. Squares are standard RPA predictions for ^{24}O. Open circles and squares are connected by dashed lines to guide the eye.

[1] M.G. Mayer, Phys. Rev. **75**, 1969 (1949)

[2] O. Haxel, J.H.D. Jensen, and H.E. Suess, Phys. Rev. **75**,

1766 (1949)
[3] C. Détraz et al., Phys. Rev. **C19**, 164 (1979)
[4] O. Tarasov et al., Phys. Lett. **B409**, 64 (1997)
[5] H. Sakurai et al., Phys. Lett. **B448**, 180 (1999)
[6] M. Stanoiu et al., Phys. Rev. **C69**, 034312 (2004)
[7] G. Audi and A. H. Wapstra, Nucl. Phys. **A595**, 409 (1995)
[8] A. Ozawa et al., Phys. Rev. Lett. **84**, 5493 (2000)
[9] T. Otsuka et al., Phys. Rev. Lett. **87**, 082502 (2001)
[10] A. P. Zuker, Phys. Rev. Lett. **91**, 179201 (2003)
[11] T. Otsuka et al., Phys. Rev. Lett. **91**, 179202 (2003)
[12] J. Dechargé and D. Gogny, Phys. Rev. **C21**, 1568 (1980)
[13] J.F. Berger, M. Girod, and D. Gogny, Comp. Phys. Comm. **63**, 365 (1991)
[14] A. Valor, P.H. Heenen, and P. Bonche, Nucl. Phys. **A671**, 145 (2000)
[15] R. Rodríguez-Guzmán, J.L. Egido, and L.M. Robledo, Phys. Lett. **B474**, 15 (2000)
[16] S. Péru, M. Girod, and J.F. Berger, Eur. Phys. J. **A9**, 35 (2000)
[17] P. Ring and P. Shuck, *The Nuclear Many-Body Problem* (Springer-Verlag, Heidelberg, 1980)
[18] D. L. Hill, and J. A. Wheeler, Phys. Rev. **89**, 1102 (1953)
[19] J. Libert, M. Girod, and J.-P. Delaroche, Phys. Rev. **C60**, 054301 (1999)
[20] K. Kumar and M. Baranger, Nucl. Phys. **A92**, 608 (1967)
[21] M. Girod, and B. Grammaticos, Phys. Rev. **C27**, 2317 (1983)
[22] D. R. Inglis, Phys. Rev. **103**, 1786 (1956)
[23] S. T. Belyaev, Nucl. Phys. **24**, 322 (1961)
[24] D. Sohler et al., Phys. Rev. **C66**, 054302 (2002)
[25] M. Girod et al., Phys. Lett. **B325**, 1 (1994)
[26] D. J. Thouless and J. G. Valatin, Nucl. Phys. **31**, 211 (1962)
[27] J. P. Blaizot and D. Gogny, Nucl. Phys. **A284**, 429 (1977)
[28] S. Raman et al., At. Nucl. Data Tables **78**, 1 (2001) and references therein